# The impact of a water wedge on a wall

By E. CUMBERBATCH†
Department of Mathematics, University of Manchester

(Received 22 June 1959)

## 1. Introduction

This paper is intended to give some indication of the impact forces of a water wave on a wall. The effect of gravity forces in the small time interval of impact considered will be small and is neglected. The shape of the wave before impact is considered to be a two-dimensional wedge which is assumed to strike a wall at right angles to its path. The wedge is assumed to be infinite in extent and to have a uniform translational velocity $V$ before impact. The choice of a wedge shape enables the problem to be formulated in terms of similarity variables $x/Vt$, $y/Vt$, where the origin of the $x$, $y$ plane is at the initial point of contact of the vertex of the wedge with the wall. The solution presented here can be easily adapted to the problem of an axi-symmetric cone of water striking a wall, but this is not pursued in the present paper.

A solution is obtained in §5 by suitably joining solutions valid at large and small distances from the wall. These solutions are obtained in §§3 and 4, respectively. The solution valid far from the wall may be regarded as an expansion beginning from the initial wedge shape. The solution valid near the wall may be regarded as an expansion beginning from a wedge having its axis along the wall and its vertex at the point of contact of the free surface with the wall. The method adopted in §5 of joining the solutions valid at large and small distances from the wall ensures continuity at the matching point of the slope and curvature of the free surface and the free surface potential. The condition of the conservation of mass is also satisfied.

A check on the method of solution is provided by the theorem that, for free surface problems with similarity, the arc length between fluid particles on the free surface is conserved. This theorem has been proved by Wagner (1932) and Garabedian (1953). The arc length of the solution obtained may be compared with the arc length of the wedge shape obtained in the absence of the wall. The difference between these arc lengths for the 22·2° and 45° semi-angle wedge examples computed is $0{\cdot}05\,Vt$ and $0{\cdot}26\,Vt$, respectively. It may therefore be inferred that the expansions and matching procedure used in this paper provide a reasonable description of the flow.

The solution valid far from the wall is obtained in §3 by assuming an expansion of the flow equations in this region. These equations are approximated to give four first-order non-linear equations which are reduced to two first-order equations, and a numerical solution is then obtained. Although the solution valid far from the wall may be inaccurate near the wall, it is used in §3 to

† At present at the California Institute of Technology, Pasadena, California.

provide a first estimate of the flow there. It is found that the wall condition of zero normal velocity cannot be satisfied at all points of the wall in this solution. However, by imposing a condition of zero total mass flow across the plane of flow, it is found that a moderate approximation to the wall condition is obtained. An estimate of the accuracy of the solution obtained in this way is provided by the condition of the conservation of mass. It is found that, of the mass displaced outside the oncoming wedge shape, 60 % is conserved for the 22·2° semi-angle wedge and 86 % for the 45° semi-angle wedge.

The solution valid near the wall is obtained in § 4, and is used to improve the description of the flow near the wall of the solution obtained in § 3. An expansion of the flow equations near the wall, similar to the expansion far from the wall but with the similarity variables interchanged, is assumed and the flow equations are again reduced to two first-order equations. This solution is then joined, in § 5, to the solution valid far from the wall. The conditions of continuity of the slope and curvature of the free surface at the matching point uniquely determine the matching of the solutions of the reduced equations. An arbitrary constant appears when the matched solution is completed in the physical plane, corresponding to an arbitrary position of the vertex of the wedge along the wall. This arbitrary constant is determined by imposing the condition of continuity of the potential on the free surface at the matching point. For a given angled wedge at infinity, the mass conservation condition is satisfied by choice of the angle at which the free surface meets the wall.

In the general problem of wave impact on a wall the total exchange of momentum with the wall up to a given time might be crudely estimated by supposing that all the fluid, which would have crossed the plane of the wall had the wall not been there, has lost all its momentum and the rest has lost none. The force on the wall could then be obtained by differentiation with respect to time. The analysis of this paper indicates that in two cases (wedges of semi-angles 45° and 22·2°) the force is greater than the value so obtained by factors 2·4 and 1·6, respectively.

## 2. Formulation

A two-dimensional wedge of water, incompressible and of density $\rho$, is taken to strike a flat wall at time $t = 0$ with velocity $V$. The axis of the wedge is perpendicular to the wall. The initial point of contact of the vertex of the wedge with the wall is taken as the origin of the $x$, $y$ plane, with the $y$-axis along the axis of the wedge and the $x$-axis along the wall. The semi-angle of the wedge is taken to be $\tan^{-1} m_1$.

The problem is formulated in terms of a velocity potential $\Phi = \Phi(x, y, t)$ which, for an irrotational flow, satisfies Laplace's equation

$$\frac{\partial^2\Phi}{\partial x^2}+\frac{\partial^2\Phi}{\partial y^2} = 0 \tag{1}$$

at any time $t$. Bernoulli's theorem states that the quantity,

$$\frac{p}{\rho}+\frac{1}{2}\left(\frac{\partial\Phi}{\partial x}\right)^2+\frac{1}{2}\left(\frac{\partial\Phi}{\partial y}\right)^2+\frac{\partial\Phi}{\partial t}, \tag{2}$$

where $p$ is the pressure at a point in the flow, depends only on the time. Boundary conditions of zero normal velocity at the wall $y = 0$ and on the line $x = 0$ are derived from the wall condition and from considerations of symmetry about the axis of the wedge, respectively. The flow far from the wall approximates to uniform translation given by

$$\frac{\partial \Phi}{\partial y} \sim -V, \quad \frac{\partial \Phi}{\partial x} \sim 0. \tag{3}$$

The potential has also to satisfy boundary conditions on the free surface $y = \eta(x, t)$, namely, that the pressure is a constant which is taken as zero, and that particles in the free surface remain there, which may be written as $(D/Dt)\,(y-\eta) = 0$. This second condition is expressed in terms of $\Phi$ as

$$\frac{\partial \Phi}{\partial y} = \frac{\partial \eta}{\partial t} + \frac{\partial \Phi}{\partial x}\frac{\partial \eta}{\partial x}. \tag{4}$$

The absence of a fundamental length in the formulation of the problem implies that a similarity solution is possible. Upon a transformation of the independent variables $x, y, t$ to

$$\lambda = \frac{x}{tV}, \quad \mu = \frac{y}{tV}, \quad t_1 = t, \tag{5}$$

the assumption of a similarity solution implies that the dependent variables are functions of $\lambda$, $\mu$ and $t_1$ in the form

$$\Phi(x, y, t) = t_1 V^2 \phi(\lambda, \mu), \quad \eta(x, t) = t_1 V \xi(\lambda). \tag{6}$$

Equation (1) may be expressed in terms of the similarity variables to show that $\phi$ also satisfies Laplace's equation

$$\frac{\partial^2 \phi}{\partial \lambda^2} + \frac{\partial^2 \phi}{\partial \mu^2} = 0. \tag{7}$$

The boundary condition (4), valid on the free surface $\mu = \xi(\lambda)$, is transformed to

$$\frac{\partial \phi}{\partial \mu} = \mu - \lambda\frac{d\mu}{d\lambda} + \frac{\partial \phi}{\partial \lambda}\frac{d\mu}{d\lambda}. \tag{8}$$

Substitution of the free surface pressure condition, $p = 0$, in Bernoulli's theorem, (2), gives that on $\mu = \xi(\lambda)$

$$\left(\frac{\partial \phi}{\partial \lambda}\right)^2 + \left(\frac{\partial \phi}{\partial \mu}\right)^2 - 2\lambda\frac{\partial \phi}{\partial \lambda} - 2\mu\frac{\partial \phi}{\partial \mu} + 2\phi = C, \tag{9}$$

where $C$ is a constant. Equation (3) for the flow far from the wall gives that

$$\frac{\partial \phi}{\partial \mu} \sim -1, \quad \frac{\partial \phi}{\partial \lambda} \sim 0, \tag{10}$$

as $\mu \to \infty$. Hence, for large $\mu$

$$\phi \sim -\mu. \tag{11}$$

Substitution of the above values for $\phi$ and its derivatives far from the wall in equation (9) yields the value of $C$ as unity provided the constant term in $\phi$ is taken to be zero. Similarly, equation (8) may be used to derive $\lambda(d\mu/d\lambda) \sim \mu+1$ for the asymptotic shape of the free surface. On integration this becomes

$$\lambda \sim m_1(\mu+1), \tag{12}$$

where $\tan^{-1} m_1$ is the semi-angle of the water wedge. This shows that for time $t > 0$, the free surface in the similarity plane is asymptotic to the wedge with vertex at $\mu = -1$ shown in figure 1. This wedge represents the position the original wedge would have reached in the absence of the wall.

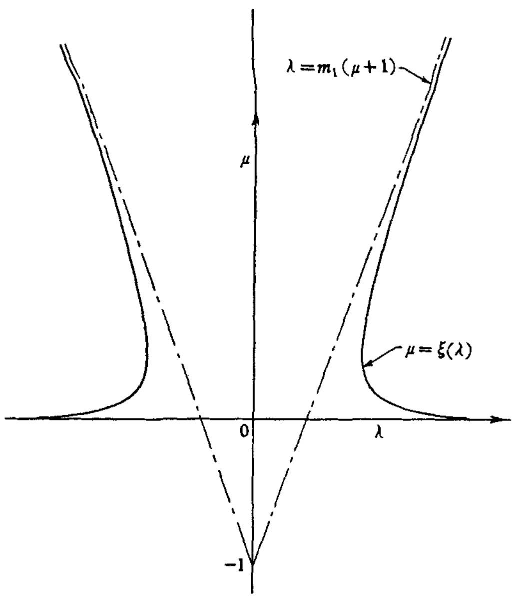


FIGURE 1. $\lambda$-$\mu$ similarity plane showing a sketch of the free surface $\mu = \xi(\lambda)$. The free surface tends at large $\mu$ to $\lambda = m_1(\mu+1)$ which represents the position the wedge would have reached in the absence of the wall.

A simplification of the equations may be made by the substitution

$$\psi(\lambda, \mu) = \phi(\lambda, \mu) - \tfrac{1}{2}(\lambda^2+\mu^2). \tag{13}$$

Equation (7) rewritten in terms of $\psi$ is

$$\frac{\partial^2\psi}{\partial\lambda^2} + \frac{\partial^2\psi}{\partial\mu^2} = -2, \tag{14}$$

and the boundary conditions (8) and (9) on the free surface $\mu = \xi(\lambda)$ may be expressed as

$$\frac{d\mu}{d\lambda} = \frac{\partial\psi}{\partial\mu}\Big/\frac{\partial\psi}{\partial\lambda}, \tag{15}$$

$$\left(\frac{\partial\psi}{\partial\lambda}\right)^2 + \left(\frac{\partial\psi}{\partial\mu}\right)^2 + 2\psi = 1, \tag{16}$$

respectively. The flow velocities may be written in terms of $\psi$ as

$$\frac{\partial \Phi}{\partial x} = V\left(\frac{\partial \psi}{\partial \lambda} + \lambda\right), \quad \frac{\partial \Phi}{\partial y} = V\left(\frac{\partial \psi}{\partial \mu} + \mu\right). \tag{17}$$

The boundary conditions of zero normal velocity on $y = 0$ and $x = 0$ are thus

$$\left(\frac{\partial \psi}{\partial \mu}\right)_{\mu=0} = 0, \quad \left(\frac{\partial \psi}{\partial \lambda}\right)_{\lambda=0} = 0. \tag{18}$$

The flow equations (14)–(18), derived in terms of $\psi(\lambda, \mu)$, are used in the following sections where two solutions are derived which are used at large and small distances from the wall.

## 3. Solution at large distances from the wall

In this section the flow equations obtained in § 2 are approximated in the region far from the wall. These equations are solved in the whole plane to provide a first approximation to the flow. It is seen that this solution is inadequate near the wall and the solution in this region is modified in later sections.

An expansion of the function $\psi(\lambda, \mu)$ defined in § 2 is sought containing as its dominant term the wedge behaviour $\psi(\lambda, \mu) \sim -\frac{1}{2}\mu^2 - \mu - \frac{1}{2}\lambda^2$ as $\mu \to \infty$, which is obtained from (11) and (13). The form

$$\psi(\lambda, \mu) = \psi_0(\mu) + \lambda^2 \psi_1(\mu) \tag{19}$$

is assumed, where

$$\psi_0 \sim -\tfrac{1}{2}\mu^2 - \mu, \quad \psi_1 \sim -\tfrac{1}{2}, \tag{20}$$

as $\mu \to \infty$. This form for $\psi$ has the same $\lambda$ dependence as the wedge solution at infinity. The form (19) satisfies the symmetrical boundary condition

$$(\partial \psi / \partial \lambda)_{\lambda=0} = 0,$$

but the wall condition

$$(\partial \psi / \partial \mu)_{\mu=0} = 0$$

is satisfied only if

$$\left(\frac{d\psi_0}{d\mu}\right)_{\mu=0} = \left(\frac{d\psi_1}{d\mu}\right)_{\mu=0} = 0. \tag{21}$$

A difficulty concerning this wall condition is encountered later in this section. On using the form (19) for $\psi$, the term independent of $\lambda$ in the flow equation (14) is

$$\psi_0'' + 2\psi_1 = -2, \tag{22}$$

where the dash denotes differentiation with respect to $\mu$. The boundary equations (15) and (16) for the free surface reduce to

$$\frac{d\mu}{d\lambda} = \frac{\psi_0'}{2\lambda\psi_1}, \tag{23}$$

$$2\psi_0 + \psi_0'^2 + \lambda^2(2\psi_0'\psi_1' + 2\psi_1 + 4\psi_1^2) = 1, \tag{24}$$

where only the lowest powers of $\lambda$ have been retained.

On making the substitution

$$\frac{d\psi_0}{d\mu} = \chi(\mu), \tag{25}$$

equation (22) reduces to the first-order equation

$$\frac{d\chi}{d\mu} = -2-2\psi_1, \tag{26}$$

and (23), (24) become

$$\frac{d\lambda}{d\mu} = \frac{2\lambda\psi_1}{\chi}, \tag{27}$$

$$\frac{d\psi_1}{d\mu} = \frac{1}{2\chi}\left(\frac{1-2\psi_0-\chi^2}{\lambda^2} - 2\psi_1 - 4\psi_1^2\right). \tag{28}$$

The independent variable $\mu$ is eliminated from equations (25), (26), (27) and (28) since it does not occur on the right-hand side of these equations. Dividing the equations (26), (27) and (28) by (25), the system reduces to

$$\frac{d\chi}{d\psi_0} = -\frac{2+2\psi_1}{\chi}, \tag{29}$$

$$\frac{d\lambda}{d\psi_0} = \frac{2\lambda\psi_1}{\chi^2}, \tag{30}$$

$$\frac{d\psi_1}{d\psi_0} = \frac{1}{2\chi^2}\left(\frac{1-2\psi_0-\chi^2}{\lambda^2} - 2\psi_1 - 4\psi_1^2\right), \tag{31}$$

where the functions $\lambda$, $\psi_1$ and $\chi$ are to be interpreted as functions of $\psi_0$. Throughout this paper the same symbol will be used to denote the same physical quantity.

Further reduction is accomplished by a transformation of the variables. The transformation corresponds to the extraction of the asymptotic wedge solution. The behaviour of $\psi_0$ and $\psi_1$ as $\mu \to \infty$ is given by (20). The behaviour of $\psi_0$ is rewritten in the form

$$\sqrt{(1-2\psi_0)} \sim 1+\mu. \tag{32}$$

The behaviour of $\chi = d\psi_0/d\mu$ as $\mu \to \infty$ follows as $\chi \sim -\sqrt{(1-2\psi_0)}$. The shape of the free surface as $\mu \to \infty$ is given by (12), which may be expressed, using (32), as $\lambda \sim m_1\sqrt{(1-2\psi_0)}$. New variables $f(\psi_0)$, $g(\psi_0)$, $z(\psi_0)$, are therefore defined by

$$\begin{aligned} \psi_1(\psi_0) &= -\tfrac{1}{2}f(\psi_0), \quad \lambda(\psi_0) = m_1\, g(\psi_0)\sqrt{(1-2\psi_0)}, \\ \chi(\psi_0) &= -z(\psi_0)\sqrt{(1-2\psi_0)}, \end{aligned} \tag{33}$$

where it follows, from the above, that as $\mu \to \infty$, $f$, $g$ and $z$ all tend to one.

Under the substitutions (33), equations (29), (30), (31) become

$$(1-2\psi_0)\frac{dz}{d\psi_0} = (f+z^2-2)/z, \tag{34}$$

$$(1-2\psi_0)\frac{dg}{d\psi_0} = g - gf/z^2, \tag{35}$$

$$(1-2\psi_0)\frac{df}{d\psi_0} = \left\{f^2 - f + \frac{1}{m_1^2 g^2}(z^2-1)\right\}\Big/ z^2. \tag{36}$$

Reduction to two equations follows immediately as the independent variable $\psi_0$ occurs only in the combination $d\psi_0/(1-2\psi_0)$ and may be eliminated.

Dividing equations (35) and (36) by (34), the following two first-order equations are obtained

$$\frac{dg}{dz} = \frac{g(f-z^2)}{z(2-f-z^2)}, \tag{37}$$

$$\frac{df}{dz} = \frac{g^2(f-f^2)+(1/m_1^2)(1-z^2)}{zg^2(2-f-z^2)}. \tag{38}$$

The equations (37), (38) are integrated numerically with the boundary conditions, $f = 1$, $g = 1$ at $z = 1$.

Numerical integration of equations (37), (38) requires the initial values of $dg/dz$, $df/dz$. As the functions on the right-hand side of (37), (38) are indeterminate at the starting point $z = 1$, an expansion

$$f = 1+f_0(z-1)+f_1(z-1)^2+f_2(z-1)^3+\ldots, \tag{39}$$

$$g = 1+g_0(z-1)+g_1(z-1)^2+g_2(z-1)^3+\ldots, \tag{40}$$

near the point $z = 1$ is assumed. This expansion is then substituted in equations (37), (38) to find the required values $f_0$, $g_0$. These are given by the equations

$$f_0 = \frac{1}{2}\left\{-1 \pm \sqrt{\left(1+\frac{8}{m_1^2}\right)}\right\}, \tag{41}$$

$$g_0 = (2-f_0)/(2+f_0). \tag{42}$$

Further coefficients in the expansions (39), (40) and details of the expansions used in the rest of this paper may be obtained from Cumberbatch (1958). Choice of the square-root sign to be taken in equation (41) for $f_0$ may be decided on inspection of the behaviour of equation (34) near $z = 1$. Substituting the expansion (39) in the right-hand side of (34) gives

$$(1-2\psi_0)\frac{dz}{d\psi_0} = (f_0+2)(z-1)+\ldots, \tag{43}$$

to the first power in $(z-1)$. Integration of (43) gives

$$\sqrt{(1-2\psi_0)} \sim (z-1)^{-1/(f_0+2)} \tag{44}$$

near $z = 1$. The value of $\sqrt{(1-2\psi_0)}$ as $\mu \to \infty$, which corresponds to $z \to 1$, may be deduced from (32) to be infinite, and it follows from (44) therefore that $(f_0+2)$ is positive. This condition is satisfied by both signs of the square root in (41) for $m_1 > 1$, corresponding to a wedge of semi-angle greater than 45°, but is satisfied only by the positive square-root sign for $m_1 \leqslant 1$. Solutions for wedges of semi-angle greater than 45° are not considered in this paper.

The initial direction of integration from the point $z = 1$ for the solution of the reduced equations (37), (38) is deduced in the following manner from the assumption that the free surface expands away from the asymptotic wedge shape in the physical plane. The slope of the free surface is obtained from (27), using (33), as

$$\frac{d\mu}{d\lambda} = \frac{z}{m_1 fg}. \tag{45}$$

On using the expansions (39) and (40), this becomes

$$\frac{d\mu}{d\lambda} = \frac{1}{m_1}\{1+(1-f_0-g_0)(z-1)+\ldots\}. \tag{46}$$

The condition that the slope $d\mu/d\lambda$ increases along the free surface proceeding towards the wall from infinity implies that the initial direction of integration in the $z$-plane is chosen so that $(z-1)$ has the same sign as $(1-f_0-g_0)$. For the 45° and 22·2° semi-angle wedges computed, $(1-f_0-g_0)$ is negative and the initial direction of integration is $z$ decreasing.

The integration should be terminated at a value of $z$ corresponding to the wall conditions (21), which may be written in terms of the reduced variables, by using equations (25), (28) and (33), as

$$\frac{d\psi_0}{d\mu} = -z\sqrt{(1-2\psi_0)} = 0, \tag{47}$$

$$\frac{d\psi_1}{d\mu} = \frac{-1}{2m_1^2 zg^2\sqrt{(1-2\psi_0)}}\{1-z^2+m_1^2g^2(f-f^2)\} = 0. \tag{48}$$

These conditions are not simultaneously satisfied. This is a weakness of the form of $\psi$, given by (19), assumed for this solution. A single condition of zero total mass flow across a plane at right angles to the flow is imposed instead. This condition may be obtained by integrating the normal velocity, given by (17), across the plane of the flow at $\mu = 0$, as

$$V\int_0^\lambda \left(\frac{\partial\psi}{\partial\mu}\right)_{\mu=0} d\lambda = V\left(\lambda\frac{d\psi_0}{d\mu}+\tfrac{1}{3}\lambda^3\frac{d\psi_1}{d\mu}\right) = 0. \tag{49}$$

Using the expressions in (47), (48) for $d\psi_0/d\mu$ and $d\psi_1/d\mu$, and equation (33) for $\lambda$, the condition (49) may be expressed in terms of the reduced variables as

$$1+5z^2+m_1^2g^2(f-f^2) = 0. \tag{50}$$

Equations (37), (38) are integrated until values $z_w, f_w, g_w$ are found which satisfy this condition. The wall is taken to be at the position in the physical plane corresponding to this point.

Numerical solutions to equations (37), (38) are obtained for the cases $m_1 = 1$ and $m_1 = 1/\sqrt{6}$, corresponding to wedges of semi-angle 45° and 22·2°, respectively. These solutions are displayed in figure 2. The numerical integration proceeds from the point $f = g = z = 1$ until the mass flow condition (50) is satisfied by values $f_w, g_w, z_w$. The values of $z_w$ obtained are small, being $z_w = 0{\cdot}041$ and $z_w = 0{\cdot}126$ for the 45° and 22·2° wedges, respectively. The wall conditions (47) and (48) are therefore satisfied approximately as $d\psi_0/d\mu$ is zero when $z = 0$ and the vanishing of $d\psi_1/d\mu$ and the mass flow across $\mu = 0$ both reduce to $1+m_1^2g^2(f-f^2) = 0$ when $z = 0$.

The solution in the physical plane is now deduced. Integration of (34) gives

$$\sqrt{(1-2\psi_0)} = k\exp\left(\int_{z_w}^{z}\frac{z\,dz}{2-f-z^2}\right), \tag{51}$$

where $k > 0$ is a constant. Equation (33) now gives $\lambda$ in terms of $z$ as

$$\lambda = m_1kg(z)\exp\left(\int_{z_w}^{z}\frac{z\,dz}{2-f-z^2}\right). \tag{52}$$

Equations (25), (33) and (34) are used to determine $d\mu/dz$ as

$$\frac{d\mu}{dz} = \frac{\sqrt{(1-2\psi_0)}}{2-f-z^2}. \tag{53}$$

Using (51), integration of (53) gives

$$\mu = k\int_{z_w}^{z} \exp\left(\int_{z_w}^{z} \frac{z\,dz}{2-f-z^2}\right)\frac{dz}{2-f-z^2}, \tag{54}$$

where the constant of integration in this equation has been chosen to give $\mu = 0$ at the wall position $z = z_w$.

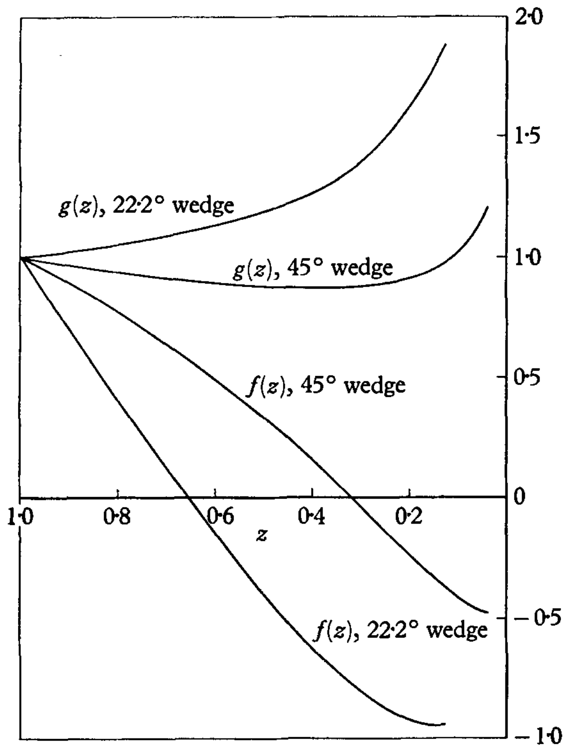


FIGURE 2. Numerical solutions to equations (37), (38) for wedges of semi-angle 45° and 22·2°. The equations are integrated from the point $f = g = z = 1$ until the mass flow condition (50) is satisfied at values $z = 0{\cdot}041$ and $z = 0{\cdot}126$, respectively.

The constant $k$ is determined from the condition that the solution has the asymptotic wedge behaviour given by (32) at large distances, which may be expressed in terms of $z$, using (51) and (54), as

$$1+k\int_{z_w}^{z} \exp\left(\int_{z_w}^{z} \frac{z\,dz}{2-f-z^2}\right)\frac{dz}{2-f-z^2} \sim k\exp\left(\int_{z_w}^{z} \frac{z\,dz}{2-f-z^2}\right) \quad \text{as} \quad z\to 1. \tag{55}$$

Since the integrals in (55) become infinite as $z \to 1$, $k$ is to be found from the equation

$$\frac{1}{k} = \lim_{z\to 1}\left\{\exp\left(\int_{z_w}^{z} \frac{z\,dz}{2-f-z^2}\right) - \int_{z_w}^{z} \exp\left(\int_{z_w}^{z} \frac{z\,dz}{2-f-z^2}\right)\frac{dz}{2-f-z^2}\right\}. \tag{56}$$

Denoting by $z^*$ a convenient point near $z = 1$, the integrals from $z_w$ to $z^*$ are taken outside the limit sign in (56). The integrals from $z_w$ to $z^*$ are evaluated by numerical integration and the integrals from $z^*$ to $z$ under the limit sign are evaluated by expanding the integrand in powers of $(z-1)$ using the expansion (39). For the 45° and 22·2° semi-angle wedge solutions computed, the values of $k$ are found to be 1·74 and 1·30, respectively.

Equations (52), (54) give the shape of the free surface in parametric form with $z$ as the parameter. The free surface shapes are drawn in figure 3 for the two wedge examples computed. The flow quantities $\psi_0$ and $\psi_1$ are given as functions

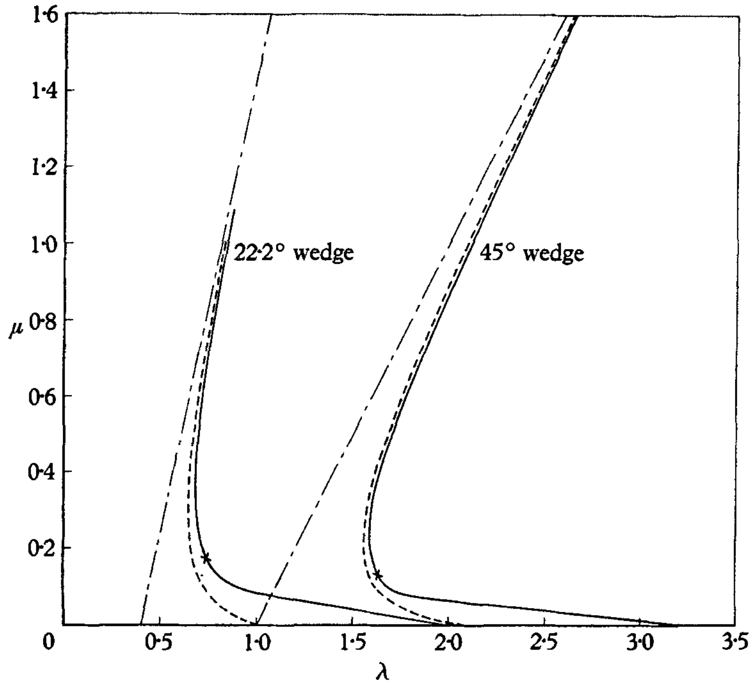


FIGURE 3. Free surface shapes for the matched solution derived in § 5 for the 45° and 22·2° semi-angle wedges are shown by the solid lines, with the matching points indicated by a cross. Broken lines indicate the position these wedges would have reached in the absence of the wall and have their vertices at $\mu = -1$. The approximate solutions derived in § 3 for these wedges are shown by dotted lines.

of $z$ by equation (51) and $\psi_1 = -\frac{1}{2}f(z)$, respectively. As $\mu$ is given as a function of $z$ by (54), the functions $\lambda$, $\psi_0$, $\psi_1$ and $z$ are tabulated as functions of $\mu$ in tables 1 and 2 for the 45° and 22·2° semi-angle wedges, respectively. The value of $\psi = \psi_0(\mu) + \lambda^2\psi_1(\mu)$ on the free surface, $\psi_F$ say, is given by the tables using the free surface $\lambda$ given there. However, $\psi$ can be evaluated at any point of the flow by using the appropriate value of $\lambda$.

The pressure on the wall due to the water wedge striking it is deduced as follows. The pressure at a point in the flow is given by Bernoulli's equation (2). Under the substitutions made in § 2, the pressure coefficient $p/\frac{1}{2}\rho V^2$ may be derived in terms of the function $\psi(\lambda, \mu)$ as

$$\frac{p}{\frac{1}{2}\rho V^2} = 1 - 2\psi - \left(\frac{\partial\psi}{\partial\lambda}\right)^2 - \left(\frac{\partial\psi}{\partial\mu}\right)^2. \tag{57}$$

Using the form of $\psi$ given by (19), this is written

$$\frac{p}{\frac{1}{2}\rho V^2} = 1-2\psi_0-\psi_0'^2-\lambda^2(2\psi_0'\psi_1'+2\psi_1+4\psi_1^2), \tag{58}$$

again retaining only $\lambda^2$ terms. The pressure distribution (58) is therefore parabolic across planes at right angles to the flow. A more convenient form of (58) is derived by obtaining the terms in the bracket on the right-hand side from

| $\mu$ | $\lambda$ | $\psi_0$ | $\psi_1$ | $\psi_F$ | $z$ |
|---|---|---|---|---|---|
| 0 | 2·09 | −1·01 | 0·236 | 0·024 | 0·041 |
| 0·006 | 2·02 | −1·01 | 0·235 | −0·046 | 0·048 |
| 0·014 | 1·94 | −1·01 | 0·231 | −0·141 | 0·061 |
| 0·026 | 1·85 | −1·01 | 0·222 | −0·249 | 0·078 |
| 0·043 | 1·76 | −1·01 | 0·205 | −0·372 | 0·102 |
| 0·070 | 1·68 | −1·02 | 0·175 | −0·524 | 0·137 |
| 0·118 | 1·60 | −1·03 | 0·115 | −0·738 | 0·2 |
| 0·204 | 1·56 | −1·07 | 0·015 | −1·032 | 0·3 |
| 0·303 | 1·57 | −1·13 | −0·080 | −1·330 | 0·4 |
| 0·422 | 1·63 | −1·23 | −0·168 | −1·679 | 0·5 |
| 0·571 | 1·74 | −1·40 | −0·249 | −2·157 | 0·6 |
| 0·773 | 1·89 | −1·65 | −0·322 | −2·807 | 0·7 |
| 1·080 | 2·17 | −2·18 | −0·388 | −4·009 | 0·8 |
| 1·701 | 2·74 | −3·51 | −0·447 | −6·863 | 0·9 |

TABLE 1

TABLES 1 AND 2. Values of the free surface shape $\lambda(\mu)$, and the flow quantities $\psi_0(\mu)$, $\psi_1(\mu)$, $z(\mu)$ for the approximate solution derived in § 3 for wedges of semi-angle 45° (table 1) and 22·2° (table 2). Values of $\psi = \psi_F$ along the free surface are also given.

| $\mu$ | $\lambda$ | $\psi_0$ | $\psi_1$ | $\psi_F$ | $z$ |
|---|---|---|---|---|---|
| 0 | 1·000 | −0·347 | 0·472 | 0·125 | 0·126 |
| 0·005 | 0·974 | −0·348 | 0·474 | 0·102 | 0·136 |
| 0·010 | 0·948 | −0·349 | 0·475 | 0·078 | 0·148 |
| 0·016 | 0·922 | −0·350 | 0·474 | 0·053 | 0·161 |
| 0·022 | 0·896 | −0·352 | 0·472 | 0·027 | 0·176 |
| 0·030 | 0·870 | −0·354 | 0·467 | 0·001 | 0·193 |
| 0·039 | 0·845 | −0·356 | 0·460 | −0·027 | 0·212 |
| 0·048 | 0·820 | −0·359 | 0·450 | −0·056 | 0·233 |
| 0·060 | 0·794 | −0·362 | 0·436 | −0·087 | 0·257 |
| 0·073 | 0·770 | −0·367 | 0·416 | −0·120 | 0·285 |
| 0·088 | 0·746 | −0·373 | 0·391 | −0·156 | 0·317 |
| 0·107 | 0·722 | −0·382 | 0·357 | −0·196 | 0·355 |
| 0·131 | 0·700 | −0·393 | 0·312 | −0·241 | 0·4 |
| 0·159 | 0·680 | −0·409 | 0·258 | −0·282 | 0·45 |
| 0·189 | 0·666 | −0·429 | 0·199 | −0·341 | 0·5 |
| 0·223 | 0·655 | −0·453 | 0·138 | −0·394 | 0·55 |
| 0·260 | 0·649 | −0·483 | 0·073 | −0·452 | 0·6 |
| 0·302 | 0·647 | −0·520 | 0·006 | −0·523 | 0·65 |
| 0·350 | 0·648 | −0·567 | −0·063 | −0·593 | 0·7 |
| 0·408 | 0·655 | −0·630 | −0·133 | −0·687 | 0·75 |
| 0·481 | 0·669 | −0·716 | −0·205 | −0·807 | 0·8 |
| 0·576 | 0·693 | −0·843 | −0·277 | −0·976 | 0·85 |
| 0·719 | 0·736 | −1·055 | −0·351 | −1·245 | 0·9 |
| 0·991 | 0·831 | −1·530 | −0·425 | −1·824 | 0·95 |

TABLE 2. For explanation see table 1.

(24), which is valid only on the free surface, in terms of the $\lambda$ co-ordinate of the free surface $\lambda_F$. Obtaining $\psi_0' = \chi$ from (33), the pressure distribution (58) is written as

$$\frac{p}{\frac{1}{2}\rho V^2} = (1-2\psi_0)(1-z^2)\left(1-\frac{\lambda^2}{\lambda_F^2}\right), \tag{59}$$

where the values of $\psi_0$, $z$ and $\lambda_F$ are given as functions of $\mu$ in tables 1 and 2 for the two wedge examples computed. The pressure distribution on the wall $\mu = 0$ is shown for these examples in figure 4.

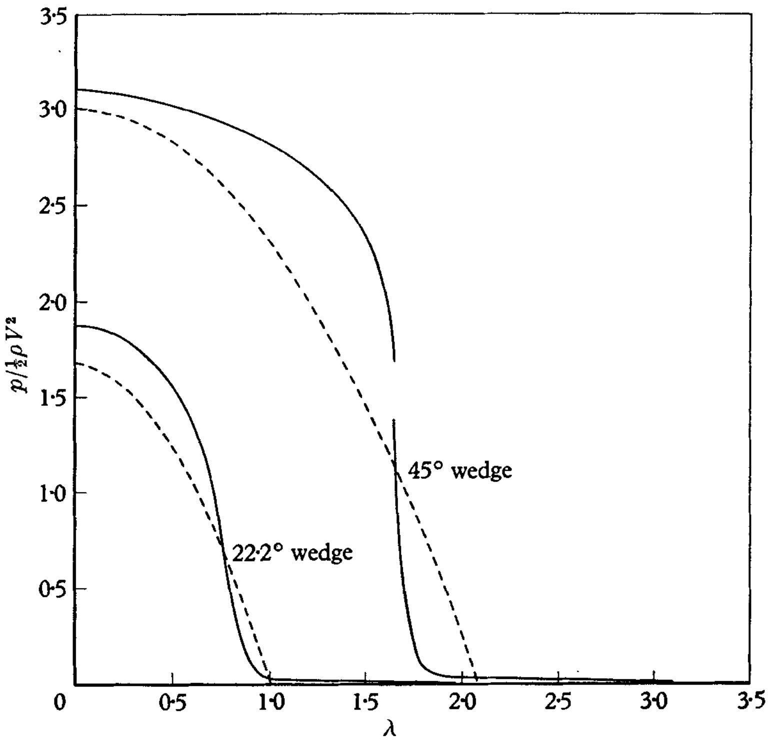


FIGURE 4. Pressure distributions on the wall for the matched solution obtained in § 5 for the 45° and 22·2° semi-angle wedges are shown by solid lines. The pressure distributions on the wall for the approximate solution of § 3 for these wedges are shown by dotted lines.

A force coefficient normalized with respect to the angle of the wedge is constructed as follows. In the absence of the wall, the momentum, per unit width of the wedge, passing $\mu = 0$ is $\rho V v$, where $v$ is the volume of fluid that has crossed $\mu = 0$ at any stage. A force $F$, derived as the rate of change of momentum across $\mu = 0$, is

$$F = \frac{d}{dt}(\rho V v) = \rho V \frac{dv}{dt}.$$

The rate of change of the volume, $dv/dt$, is expressed as $VA$, where $A$ is the area of the wedge at $\mu = 0$ at any stage. The force on a wall obstructing the flow of the wedge is the integral of the pressure over the wetted area $A_w$. A normalized force coefficient $C_F$ is therefore defined as

$$C_F = \frac{1}{\rho V^2 A}\int_{A_w} p\,dA = \frac{1}{2m_1}\int_0^{\lambda_w} \frac{p}{\frac{1}{2}\rho V^2}\,d\lambda, \tag{60}$$

where $\lambda_w$ is the point of contact of the free surface with the wall. The force coefficients obtained in this way for the 45° and 22·2° semi-angle wedges are $C_F = 2{\cdot}1$ and $C_F = 1{\cdot}4$, respectively.

An estimate of the accuracy of the solution obtained using the approximate equations (37), (38) is provided by the condition of the conservation of mass. In the absence of the wall the fluid occupies the wedge with vertex at $\mu = -1$, as shown in figure 1. The area of this portion of the wedge in $\mu < 0$ is $\frac{1}{2}m_1$. In a flow obstructed by the wall, therefore, the area of fluid lying between the free surface and the wedge $\lambda = m_1(\mu+1)$ is equal to $\frac{1}{2}m_1$ in an ideal solution. This area is

$$\int_0^\infty \{\lambda - m_1(\mu+1)\}\, d\mu. \tag{61}$$

Transforming to the reduced variables by obtaining the free surface $\lambda$ from (52) and $\mu$ from (54), the area (61) is expressed as

$$m_1 k \int_{z_w}^{z} \left\{ kg(z) \exp\left(\int_{z_w}^{z} \frac{z\,dz}{2-f-z^2}\right) - 1 - k \int_{z_w}^{z} \exp\left(\int_{z_w}^{z} \frac{z\,dz}{2-f-z^2}\right) \frac{dz}{2-f-z^2} \right\}$$
$$\times \exp\left(\int_{z_w}^{z} \frac{z\,dz}{2-f-z^2}\right) \frac{dz}{2-f-z^2}. \tag{62}$$

This integral is treated in a similar manner to the integral (56) defining $k$. It may be noted that the singular parts of the integrals in the curly bracket in (62) cancel due to the choice of $k$ given in (56). For the 45° and 22·2° wedges, the integral (62) has the values 0·432 and 0·123 which are to be compared with the values of $\frac{1}{2}m_1$, namely, 0·5 and 0·204. These values imply that the solution obtained from the approximate equations (37), (38) valid at large distances from the wall is inadequate in predicting the flow near the wall. The simple $\lambda^2$ dependence assumed for $\psi$ in (19) is unable to describe the slope of the free surface near the wall. A more accurate solution in this domain is desired. Such a solution is examined in the next section, and will allow a suitable matching with the solution valid at large distances from the wall.

## 4. Solution near the tip

In this section a solution is obtained which describes the flow in a region near the point of contact, $\lambda_w$, of the free surface with the wall. The solution is derived as the expansion beginning from the vertex of a wedge having its axis along the wall and its vertex at $\lambda = \lambda_w$. The semi-angle of this wedge is the angle between the tangent to the free surface at the point of contact and the wall, which is taken to be $\tan^{-1} m_2$. It is to be noted that the position $(\lambda_w)$ and the angle of the wedge determined by $m_2$ are as yet arbitrary. In the next section it will be described how $\lambda_w$, $m_2$ may be determined to give a good matching of the solution of this section with the solution of §3 valid at large distances from the wall.

An expansion of $\psi(\lambda, \mu)$ in the form

$$\psi(\lambda, \mu) = \Psi_0(\lambda) + \mu^2 \Psi_1(\lambda) \tag{63}$$

is assumed near $\mu = 0$. This form satisfies the wall boundary condition $(\partial\psi/\partial\mu)_{\mu=0} = 0$. The expansion (63) is analogous to the expansion (19) used in §3, with the $\lambda$, $\mu$ axes interchanged. The equations resulting from the substitution of the expansion (63) in the flow equations are therefore obtained by analogy with equations (22)–(31), $\lambda$ and $\mu$ being interchanged and capitals replacing small symbols for the dependent variables.

Reduction of the three equations corresponding to (29), (30) and (31) is effected by extracting the tip wedge solution. The slope of the free surface at the tip, $\lambda_w$, is $-m_2$ and hence

$$\mu \sim m_2(\lambda_w - \lambda) \quad \text{as} \quad \mu \to 0. \tag{64}$$

Corresponding to (20), the flow near the tip is given by

$$\Psi_0 \sim \tfrac{1}{2} - \tfrac{1}{2}(\lambda_w - \lambda)^2, \quad \Psi_1 \sim -\tfrac{1}{2}. \tag{65}$$

The behaviour of $\Psi_0$ is rewritten as

$$\sqrt{(1-2\Psi_0)} \sim \lambda_w - \lambda \quad \text{as} \quad \mu \to 0. \tag{66}$$

New variables $F(\Psi_0)$, $G(\Psi_0)$ and $Z(\Psi_0)$ are defined by the equations

$$\Psi_1(\Psi_0) = -\tfrac{1}{2}F(\Psi_0), \quad \mu(\Psi_0) = m_2\, G(\Psi_0)\sqrt{(1-2\Psi_0)},$$
$$\mathrm{X}(\Psi_0) = Z(\Psi_0)\sqrt{(1-2\Psi_0)}, \tag{67}$$

where $\mathrm{X} = d\Psi_0/d\lambda$. It follows from (64), (65) and (66) that as $\mu \to 0$, $F$, $G$ and $Z$ all tend to one. A sign change occurring in the last equation in (67) contains the only difference from the analogous transformation (33). The equations (37), (38) are even in $z$ and are not affected by a sign change in the last term in (33). The substitutions (67) therefore lead to equations which are identical with (37), (38) with $F$, $G$ and $Z$ replacing $f$, $g$ and $z$, namely

$$\frac{dG}{dZ} = \frac{G(F-Z^2)}{Z(2-F-Z^2)}, \tag{68}$$

$$\frac{dF}{dZ} = \frac{G(F-F^2)+(1/m_2^2)(1-Z^2)}{ZG^2(2-F-Z^2)}. \tag{69}$$

Initial values of $dG/dZ$ and $dF/dZ$ are determined by expansions of $F$ and $G$ analogous to (39), (40). Choice of the square root sign to be taken in the equation for $F_0 = (dF/dZ)_{Z=1}$, corresponding to (41), is decided from the behaviour near $Z = 1$ of the equation corresponding to (34). The value of $\sqrt{(1-2\Psi_0)}$ at the tip may be determined to be zero from (66). A negative value of $(F_0+2)$ is desired to satisfy this condition, and this is only attained when $m_2 < 1$ and by a choice of the negative square-root sign in the equation for $F_0$. The direction of integration from the point $Z = 1$ is deduced from the assumption that the required solution expands away from the tip wedge shape. The slope of the free surface is given by the equation corresponding to (27). Using the substitutions (67) this equation is expressed as

$$\frac{d\mu}{d\lambda} = -m_2\frac{FG}{Z}. \tag{70}$$

Expanding near $Z = 1$,

$$\frac{d\mu}{d\lambda} = -m_2\{1-(1-F_0-G_0)(Z-1)+\ldots\}, \tag{71}$$

where $G_0 = (dG/dZ)_{Z=1}$. The direction of integration is chosen such that $(Z-1)$ has the opposite sign to $(1-F_0-G_0)$.

Equations (68), (69) may now be integrated numerically to provide the solution corresponding to the expansion away from the wedge $\mu = m_2(\lambda_w - \lambda)$. Numerical solutions of (68), (69) for the cases $m_2 = \frac{1}{19}, \frac{1}{12}$, corresponding to

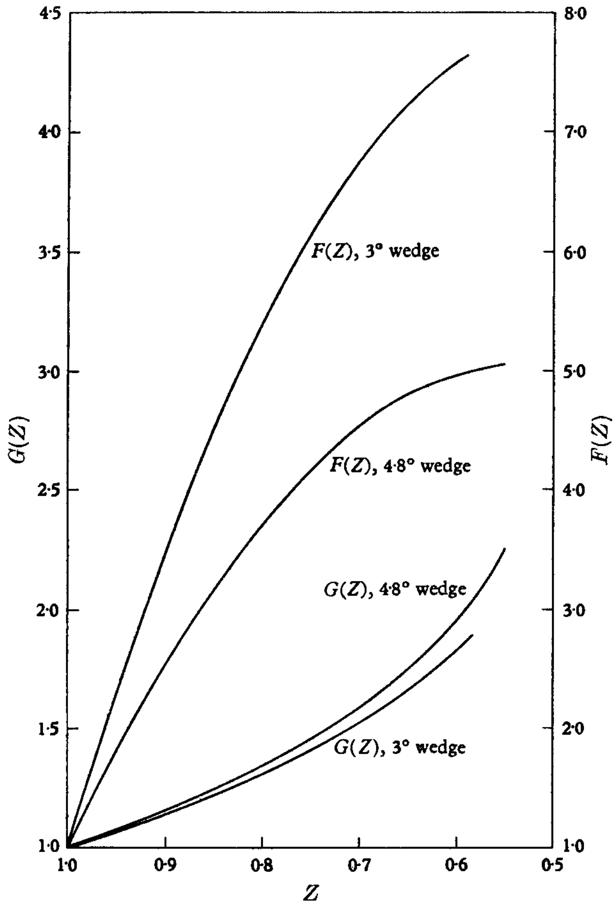


FIGURE 5. Numerical solutions to equations (68), (69) for wedges of semi-angle 3° and 4·8°.

wedges of semi-angle 3·0°, 4·8°, respectively, are shown in figure 5. The solution is valid in the tip of fluid near the point of contact of the free surface with the wall and is used to improve the accuracy near the wall of the solution obtained in § 3. The procedure for matching these solutions is discussed in § 5. The solution near the tip cannot be completed in the physical plane until the value of $Z$ at the matching point is known. Denote this by $Z_j$.

Transformation to the physical plane of the solution of equations (68), (69) is inferred by analogy with equations (51), (52), rewritten with $\lambda$ and $\mu$ interchanged, capitals replacing small symbols for the flow variables and $Z_j$ replacing $z_w$ as the lower limit of integration. Hence, using (51), $\sqrt{(1-2\Psi_0)}$ is given by

$$\sqrt{(1-2\Psi_0)} = K\exp\left(\int_{Z_j}^{Z}\frac{Z\,dZ}{2-F-Z^2}\right), \tag{72}$$

where $K > 0$ is a constant; and using the substitutions (67), it follows that

$$\mu = m_2 K G(Z)\exp\left(\int_{Z_j}^{Z}\frac{Z\,dZ}{2-F-Z^2}\right). \tag{73}$$

The equation for $d\lambda/dZ$ in the solution valid near the tip is derived by analogy with (53), but with a sign change resulting from the sign difference in the last equations of the substitutions (33) and (67). The equation for $\lambda$ is

$$\lambda_w - \lambda = K\int_1^Z \exp\left(\int_{Z_j}^{Z}\frac{Z\,dZ}{2-F-Z^2}\right)\frac{dZ}{2-F-Z^2}, \tag{74}$$

where the constant of integration has been chosen so that $\lambda = \lambda_w$ at $\mu = 0$. An expansion is required to obtain the contribution near $Z = 1$ to the integral in (74) since the integrand is singular at $Z = 1$.

Equations (73), (74) give the free surface shape in parametric form for the solution valid near the tip. The function $\psi = \Psi_0(\lambda)+\mu^2\Psi_1(\lambda)$ can now be determined at any point in the flow by using the appropriate value of $\mu$ and obtaining $\Psi_0(Z)$ from (72) and $\Psi_1(Z)$ from (67), $Z$ being obtained in terms of $\lambda$ from (74). This completes the formal description of the flow in the tip, but no numerical values can be given until the procedure for matching the tip flow with the solution in §3 is given in §5.

## 5. Matching of solutions

In this section, details are given of how the solutions derived in the previous sections may be joined together in as smooth a manner as possible. It is shown that a matching point exists at which the slope and curvature of the free surface are continuous, the function $\psi$ is continuous along the free surface and the mass conservation law is satisfied. A check on the accuracy of the method used is provided by the condition that the arc length between particles in the free surface is conserved.

Presupposing that a matching point of the two solutions has been chosen and denoting this point by the suffix $j$, the solution at large distances from the wall is given by the solution derived in §3 with $z_j$ replacing $z_w$, as it is not now intended to use this solution right up to the wall. The constant $k$ occurring in §3 depends on the choice of $z_w$ and therefore needs to be replaced by $k'$ which depends on $z_j$. The value of $\lambda$ at the matching point is given by (52) as

$$\lambda_j = m_1 k' g_j. \tag{75}$$

The formula for $\mu$ corresponding to (54) becomes

$$\mu = \mu_j + k'\int_{z_j}^{z}\exp\left(\int_{z_j}^{z}\frac{z\,dz}{2-f-z^2}\right)\frac{dz}{2-f-z^2}. \tag{76}$$

The condition that the solution at large distances from the wall has the asymptotic wedge behaviour given by (32) is expressed as

$$1+\mu_j+k'\int_{z_j}^{z}\exp\left(\int_{z_j}^{z}\frac{z\,dz}{2-f-z^2}\right)\frac{dz}{2-f-z^2}\sim k'\exp\left(\int_{z_j}^{z}\frac{z\,dz}{2-f-z^2}\right)\quad \text{as}\quad z\to 1. \tag{77}$$

This equation is used to find a relation between $k'$ and $\mu_j$ by expressing it in the form corresponding to (56) with $(1/k')(1+\mu_j)$ replacing $1/k$ on the left-hand side and $z_j$ replacing $z_w$ as the lower limit in the integrals on the right-hand side. The limit as $z\to 1$ of these integrals is deduced by an expansion near $z=1$ in a similar manner to the derivation of $k$. Thus a given angle wedge at infinity is uniquely described up to any chosen join-up point $\mu_j$.

The solution valid near the tip has been given in §4. The flow variables and the shape of the free surface are given there in terms of the constants $m_2$, $\lambda_w$, $Z_j$ and $K$. The $\mu$-co-ordinate of the matching point is deduced from (73) as

$$\mu_j = m_2 K G_j. \tag{78}$$

It is seen that the co-ordinates of the matching point $\lambda_j$, $\mu_j$ are given by (75) and (78) in terms of the constants $k'$, $K$, $m_2$, $z_j$ and $Z_j$. The condition (77) for the correct asymptotic wedge behaviour gives a relation between $\mu_j$, $k'$ and $z_j$. The value of $\lambda$ at the wall, $\lambda_w$, is given by (74) on substituting $\lambda=\lambda_j$ and $Z=Z_j$, in terms of $K$, $\lambda_j$ and $Z_j$. Thus there are four undetermined constants, which are taken to be $K$, $m_2$, $z_j$ and $Z_j$.

The condition of the continuity at the matching point of the potential on the free surface is imposed. That is, the expansions $\psi_0(\mu)+\lambda^2\psi_1(\mu)$ and $\Psi_0(\lambda)+\mu^2\Psi_1(\lambda)$ are to have the same value at the matching point. The values at the matching point for the two expansions are deduced from the sets of equations (33), (51), (76) and (67), (72), (73), respectively, to give

$$1-k'^2-m_1^2k'^2f_jg_j^2 = 1-K^2-m_2^2K^2F_jG_j^2. \tag{79}$$

This equation is regarded as determining $K$, the positive value being taken, leaving the constants $m_2$, $z_j$, $Z_j$, still arbitrary.

The matching of the two solutions valid at large and small distances from the wall has now been effected in terms of the matching points $z_j$, $Z_j$ of the reduced equations and $m_2$, the angle at which the free surface meets the wall. The method used in choosing $z_j$, $Z_j$ will now be explained. Conditions of the continuity of slope and curvature of the free surface at the matching point of the two solutions are imposed. The slope of the free surface in terms of the reduced variables of the solutions valid at large distances from the wall and near the tip are given in (45) and (70) as

$$\frac{d\mu}{d\lambda}=\frac{z}{m_1 fg}, \tag{80}$$

$$\frac{d\mu}{d\lambda}=-m_2\frac{FG}{Z}, \tag{81}$$

respectively. The second derivative of the free surface at a matching point for the two solutions may be deduced to be

$$\frac{d^2\mu}{d\lambda^2} = \frac{m_1}{k'gz^2}\left\{g^2(f^2-f)+\frac{1}{m_1^2}(1-z^2)\right\}, \tag{82}$$

$$\frac{d^2\mu}{d\lambda^2} = \frac{Z}{Km_2^2G^4F^3}\left\{G^2(F^2-F)+\frac{1}{m_2^2}(1-Z^2)\right\}. \tag{83}$$

By equating the expressions for the first and second derivatives, values of $z_j$, $Z_j$ may be found at which continuity of the first and second derivatives of the free surface is satisfied. It is to be noticed that unfortunately the supplementary integrations involved in finding the constants of integration $k'$, $K$ have to be undertaken before the values of the second derivatives at each side of the matching point may be found. This makes the solution of (82), (83) numerically tedious. The procedure adopted to determine the $z_j$, $Z_j$ which give the same value for the functions on the right-hand sides of equations (80), (81) and of (82), (83) is as follows. A first estimate of the slope of the free surface at the matching point is obtained by assuming that it is mid-way between the slope of the wedge at large distances and the slope of the free surface at the wall. Values of the matching points $z_j$, $Z_j$ in the reduced planes of the solutions may then be determined from equations (80), (81). The supplementary integrations necessary to obtain $k'$, $K$ are then performed and values of the second derivative of the free surface at each side of the matching point are calculated from (82), (83). From these values a better estimate for the slope of the free surface at the matching point is obtained. In this way continuity of the first and second derivatives of the free surface at the matching point was achieved to three significant figures.

The solution is now determined apart from the value of $m_2$. The condition of the conservation of mass is satisfied by choice of $m_2$. In the $\lambda$, $\mu$ plane this condition may be seen to be the condition that the area contained between the free surface and wedge shape given by $\lambda = m_1(\mu+1)$ is equal to the area of the part of the wedge lying in the negative $\mu$-plane. This condition may be stated as

$$\tfrac{1}{2}m_1 = \int_{\mu_j}^{\infty}\{\lambda - m_1(\mu+1)\}\,d\mu + \mu_j\lambda_j - \tfrac{1}{2}m_1\mu_j(2+\mu_j) + \int_{\lambda_j}^{\lambda_w}\mu\,d\lambda, \tag{84}$$

where the first integral on the right-hand side is the area outside the wedge in $\mu \geqslant \mu_j$, the other integral is the area outside the wedge in $\lambda \geqslant \lambda_j$ and the middle terms give the area of the part lying outside the wedge in the rectangle $0 \leqslant \lambda \leqslant \lambda_j$, $0 \leqslant \mu \leqslant \mu_j$. Transformation of the integrals in (84) to the reduced variables may be deduced for the first integral by use of equations (52) and (76), and for the second integral by use of (73), (74). After dividing by $m_1$, equation (84) may then be written

$$\begin{aligned}\tfrac{1}{2} = k'\int_{z_j}^{z}&\left\{k'g(z)\exp\left(\int_{z_j}^{z}\frac{z\,dz}{2-f-z^2}\right)-\mu_j-1-k'\int_{z_j}^{z}\exp\left(\int_{z_j}^{z}\frac{z\,dz}{2-f-z^2}\right)\frac{dz}{2-f-z^2}\right\}\\ &\times\exp\left(\int_{z_j}^{z}\frac{z\,dz}{2-f-z^2}\right)\frac{dz}{2-f-z^2}+\frac{u_j\lambda_j}{m_1}-\tfrac{1}{2}\mu_j(2+\mu_j)\\ &-K^2\frac{m_2}{m_1}\int_{Z_j}^{1}G(Z)\exp\left(2\int_{Z_j}^{Z}\frac{Z\,dZ}{2-F-Z^2}\right)\frac{dZ}{2-F-Z^2}.\end{aligned} \tag{85}$$

The contribution near $z = 1$ to the first integral on the right-hand side is derived using the expansions (39), (40). An expansion near $Z = 1$ in the last integral in (85) is needed since the integrand becomes infinite at $Z = 1$. The integral may be obtained numerically up to $Z = Z^*$, a point near $Z = 1$. The integral is expanded between $Z = Z^*$ and $Z = 1$, using the expansions for $F$, $G$ corresponding to those derived for $f$, $g$ in §3.

| $\mu$ | $\lambda$ | $\Psi_0$ | $\Psi_1$ | $\psi_F$ | $Z$ |
|---|---|---|---|---|---|
| 0 | 1·975 | 0·5 | −0·5 | 0·5 | 1 |
| 0·080 | 1·026 | 0·050 | −0·586 | 0·046 | 0·99 |
| 0·085 | 0·981 | 0·007 | −0·671 | −0·002 | 0·98 |
| 0·088 | 0·953 | −0·020 | −0·754 | −0·025 | 0·97 |
| 0·091 | 0·934 | −0·039 | −0·835 | −0·046 | 0·96 |
| 0·094 | 0·918 | −0·055 | −0·914 | −0·063 | 0·95 |
| 0·096 | 0·904 | −0·069 | −0·991 | −0·078 | 0·94 |
| 0·105 | 0·866 | −0·108 | −1·281 | −0·122 | 0·90 |
| 0·114 | 0·837 | −0·136 | −1·540 | −0·156 | 0·86 |
| 0·123 | 0·815 | −0·157 | −1·770 | −0·184 | 0·82 |
| 0·133 | 0·796 | −0·175 | −1·969 | −0·210 | 0·78 |
| 0·144 | 0·778 | −0·191 | −2·137 | −0·235 | 0·74 |
| 0·157 | 0·762 | −0·204 | −2·275 | −0·260 | 0·70 |
| 0·171 | 0·747 | −0·217 | −2·382 | −0·287 | 0·66 |

TABLE 3(i)

| $\mu$ | $\lambda$ | $\psi_0$ | $\psi_1$ | $\psi_F$ | $z$ |
|---|---|---|---|---|---|
| 0·171 | 0·747 | −0·475 | 0·338 | −0·287 | 0·374 |
| 0·186 | 0·734 | −0·483 | 0·312 | −0·315 | 0·4 |
| 0·215 | 0·714 | −0·501 | 0·258 | −0·369 | 0·45 |
| 0·247 | 0·698 | −0·522 | 0·199 | −0·425 | 0·5 |
| 0·282 | 0·688 | −0·549 | 0·138 | −0·484 | 0·55 |
| 0·321 | 0·681 | −0·581 | 0·073 | −0·547 | 0·6 |
| 0·365 | 0·678 | −0·623 | 0·006 | −0·620 | 0·65 |
| 0·416 | 0·680 | −0·674 | −0·063 | −0·703 | 0·7 |
| 0·478 | 0·688 | −0·744 | −0·133 | −0·806 | 0·75 |
| 0·553 | 0·702 | −0·838 | −0·205 | −0·939 | 0·8 |
| 0·653 | 0·727 | −0·978 | −0·277 | −1·124 | 0·85 |
| 0·803 | 0·772 | −1·211 | −0·351 | −1·421 | 0·9 |
| 1·088 | 0·872 | −1·734 | −0·425 | −2·058 | 0·95 |

TABLE 3(ii)

TABLES 3 AND 4. Values of the flow variables for the matched solution obtained in §5 for the 22·2° (table 3) and 45° (table 4) semi-angle wedges. The first half of each table is to be interpreted as giving $\Psi_0$, $\Psi_1$, $Z$ and the free surface $\mu$ as functions of $\lambda$ in the region $\lambda_j \leqslant \lambda \leqslant \lambda_w$ for the solution near the tip. The second half of each table is to be interpreted as giving $\psi_0$, $\psi_1$, $z$ and the free surface $\lambda$ as functions of $\mu$ in the region $\mu \geqslant \mu_j$ for the solution far from the wall. Values of $\psi = \psi_F$ on the free surface are given in both regions.

The following procedure to determine $m_2$ is used. A first estimate of the tip angle is given by the angle between the free surface and the wall at the point of contact obtained in the approximate solution in §3. The right-hand side of equation (85) is then evaluated for the matched solution obtained using this tip angle and this value then indicates a better value for the tip angle, an under-estimate for the mass implying that a smaller tip angle is required.

A solution was obtained in the manner described above for 22·2° and 45° semi-angle wedges. The mass conservation condition was satisfied to two significant figures by a choice of the tip angles 4·8° and 3°, respectively. The slope and curvature of the free surface were matched to three significant figures. The

| $\mu$ | $\lambda$ | $\Psi_0$ | $\Psi_1$ | $\psi_F$ | $Z$ |
|---|---|---|---|---|---|
| 0 | 3·201 | 0·5 | −0·5 | 0·5 | 1 |
| 0·072 | 1·851 | −0·410 | −0·636 | −0·413 | 0·99 |
| 0·075 | 1·813 | −0·462 | −0·768 | −0·466 | 0·98 |
| 0·077 | 1·790 | −0·493 | −0·899 | −0·498 | 0·97 |
| 0·079 | 1·773 | −0·516 | −1·026 | −0·522 | 0·96 |
| 0·080 | 1·760 | −0·534 | −1·151 | −0·541 | 0·95 |
| 0·082 | 1·749 | −0·549 | −1·273 | −0·557 | 0·94 |
| 0·083 | 1·739 | −0·562 | −1·392 | −0·571 | 0·93 |
| 0·085 | 1·731 | −0·573 | −1·509 | −0·584 | 0·92 |
| 0·086 | 1·724 | −0·583 | −1·623 | −0·595 | 0·91 |
| 0·088 | 1·717 | −0·592 | −1·735 | −0·606 | 0·90 |
| 0·094 | 1·694 | −0·622 | −2·153 | −0·641 | 0·86 |
| 0·100 | 1·676 | −0·644 | −2·528 | −0·670 | 0·82 |
| 0·107 | 1·661 | −0·662 | −2·859 | −0·695 | 0·78 |
| 0·115 | 1·648 | −0·678 | −3·145 | −0·719 | 0·74 |
| 0·123 | 1·636 | −0·692 | −3·388 | −0·743 | 0·70 |
| 0·133 | 1·625 | −0·703 | −3·585 | −0·767 | 0·66 |
| 0·134 | 1·624 | −0·704 | −3·594 | −0·768 | 0·658 |

TABLE 4 (i)

| $\mu$ | $\lambda$ | $\psi_0$ | $\psi_1$ | $\psi_F$ | $z$ |
|---|---|---|---|---|---|
| 0·134 | 1·624 | −1·073 | 0·116 | −0·768 | 0·199 |
| 0·135 | 1·623 | −1·073 | 0·115 | −0·770 | 0·2 |
| 0·176 | 1·593 | −1·090 | 0·065 | −0·925 | 0·25 |
| 0·221 | 1·581 | −1·112 | 0·015 | −1·075 | 0·3 |
| 0·269 | 1·583 | −1·140 | −0·033 | −1·223 | 0·35 |
| 0·321 | 1·597 | −1·176 | −0·080 | −1·380 | 0·4 |
| 0·378 | 1·621 | −1·221 | −0·125 | −1·549 | 0·45 |
| 0·442 | 1·655 | −1·277 | −0·168 | −1·737 | 0·5 |
| 0·512 | 1·700 | −1·348 | −0·210 | −1·955 | 0·55 |
| 0·593 | 1·757 | −1·438 | −0·249 | −2·207 | 0·6 |
| 0·686 | 1·829 | −1·554 | −0·287 | −2·514 | 0·65 |
| 0·797 | 1·920 | −1·709 | −0·322 | −2·895 | 0·7 |
| 0·932 | 2·037 | −1·920 | −0·356 | −3·397 | 0·75 |
| 1·106 | 2·192 | −2·226 | −0·388 | −4·090 | 0·8 |
| 1·345 | 2·414 | −2·707 | −0·418 | −5·142 | 0·85 |
| 1·717 | 2·767 | −3·584 | −0·447 | −7·007 | 0·9 |
| 2·484 | 3·504 | −5·846 | −0·474 | −11·666 | 0·95 |

TABLE 4 (ii). For explanation see legend to table 3.

values of $z_j$, $Z_j$, $k'$, $K$ were 0·374, 0·66, 1·40, 1·20 and 0·199, 0·658, 1·77, 1·55, for the 22·2° and 45° wedges, respectively. The co-ordinates $\lambda_j$, $\mu_j$ of the matching point were 0·747, 0·171 and 1·624, 0·134, respectively. The shape of the free surfaces for the solutions joined in this way is shown in figure 3, with the matching points indicated. Tables 3 and 4 give the values of the flow variables for the solutions matched, $\Psi_0$, $\Psi_1$ and $Z$ being given as functions of $\lambda$ for the flow in the region $\lambda_j \leqslant \lambda \leqslant \lambda_w$, and $\psi_0$, $\psi_1$ and $z$ given as functions of $\mu$ for the flow in the region $\mu \geqslant \mu_j$. The corresponding free surface values of $\lambda$ and $\mu$ are given. The values of $\psi = \psi_F$ on the free surface are also given, using (19) or (63) in the appropriate regions of the flow and using the free surface values of $\lambda$, $\mu$.

The flow in the rectangle bounded by the lines $\lambda = 0$, $\lambda_j$ and $\mu = 0$, $\mu_j$ indicated as region III in figure 6 is not deduced in the solution presented above. The solution (19) at large distances from the wall is valid in the flow region I from $\mu = \mu_j$ to $\mu = \infty$ and the solution (63) near the wall is valid in region II bounded by the lines $\lambda = \lambda_j$ and $\lambda = \lambda_w$. However, the solution in region III

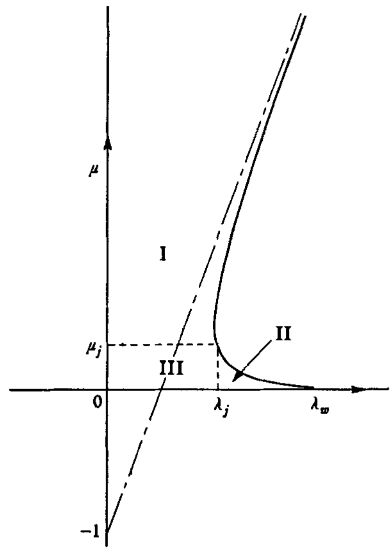


FIGURE 6. Sketch of the matched solution obtained in §5. The solution far from the wall obtained in §3 is valid in region I and the solution near the wall obtained in §4 is valid in region II.

may be obtained by a relaxation method, using the appropriate solution (19) or (63) on the boundaries adjacent to region III, together with the boundary conditions (18) on the other two boundaries. The pressure distribution on the wall in the range $0 \leqslant \lambda \leqslant \lambda_j$ may then be determined from (57). The pressure distribution between the $\lambda$-co-ordinates, $\lambda_j$ and $\lambda_w$, may be derived from the solution valid near the tip. The pressure coefficient $p/\frac{1}{2}\rho V^2$ on the wall $\mu = 0$ in this $\lambda$ range may be deduced from equation (57), making the substitution (63) for $\psi$, as

$$\frac{p}{\frac{1}{2}\rho V^2} = 1-2\Psi_0'-\Psi_0'^2 = (1-2\Psi_0')(1-Z^2) \tag{86}$$

in terms of the reduced variables, using (67). The pressure distribution on the wall over the whole range $0 \leqslant \lambda \leqslant \lambda_w$ obtained in this manner is shown in figure 4. In this description of the flow the pressure on the wall is discontinuous at $\lambda = \lambda_j$ due to its dependence on $d\psi/d\lambda$, which has not been matched between regions II and III of figure 4. For the 22·2° wedge this pressure jump is indiscernible, but for the 45° wedge the jump in $p/\frac{1}{2}\rho V^2$ is 0·321—about 10 % of the total variation along the wall. The force coefficient (60) using this pressure distribution has the values 2·4 and 1·6 for the 45° and 22·2° semi-angle wedges, respectively.

The condition of the conservation of arc length along the free surface is used to provide a check on the accuracy of the solution obtained by the matching procedure described above. The theorem that the arc length of the free surface in a two-dimensional similarity flow is conserved was discovered independently by Wagner and Garabedian. The arc length conservation condition is formulated in the $\lambda$, $\mu$ similarity plane by relating the arc length of the free surface for the solution obtained to the arc length of the free surface of the wedge shape $\lambda = m_1(\mu+1)$ obtained in the absence of the wall. Since these arc lengths are infinite the condition is derived using a technique similar to the one involved in finding $k$ from (55). Let $\mu^*$ be the $\mu$-co-ordinate corresponding to $z^*$. The parts of the arc lengths to be compared in the range from $\mu^*$ to infinity are collected together and an expansion found for their difference. The arc length condition is therefore put in the form

$$(\mu^*+1)\sqrt{(1+m_1^2)} = \int_{\mu^*}^{\infty}\left\{\sqrt{\left[1+\left(\frac{d\lambda}{d\mu}\right)^2\right]}-\sqrt{(1+m_1^2)}\right\}d\mu + \int_{\mu_j}^{\mu^*}\sqrt{\left\{1+\left(\frac{d\lambda}{d\mu}\right)^2\right\}}\,d\mu + \int_{\lambda_j}^{\lambda_w}\sqrt{\left\{1+\left(\frac{d\mu}{d\lambda}\right)^2\right\}}\,d\lambda, \quad (87)$$

where the arc lengths in the range $\mu^*$ to infinity of the solution and the wedge are to be found in the first integral on the right-hand side. The remainder of the arc length of the wedge is on the left-hand side and the remainder of the arc length of the solution is given in the last two integrals on the right-hand side which represent the contributions from the two sides of the matching point. Equation (87) is obtained in terms of the reduced variables, using (45) for $d\lambda/d\mu$ and (76) for $d\mu/dz$ for the solution between infinity and $\mu_j$, and using (70) for $d\mu/d\lambda$ and (74) for $d\lambda/dZ$ for the solution between $\lambda_j$ and $\lambda_w$ to give

$$\begin{aligned}(\mu^*+1)\sqrt{(1+m_1^2)} = {} & k'\int_{z^*}^{1}\left\{\sqrt{\left(1+\frac{m_1^2f^2g^2}{z^2}\right)}-\sqrt{(1+m_1^2)}\right\}\exp\left(\int_{z_j}^{z}\frac{z\,dz}{2-f-z^2}\right)\frac{dz}{2-f-z^2} \\ & + k'\int_{z_j}^{z^*}\sqrt{\left(1+\frac{m_1^2f^2g^2}{z^2}\right)}\exp\left(\int_{z_j}^{z}\frac{z\,dz}{2-f-z^2}\right)\frac{dz}{2-f-z^2} \\ & - K\int_{Z_j}^{1}\sqrt{\left(1+\frac{m_2^2F^2G^2}{Z^2}\right)}\exp\left(\int_{Z_j}^{Z}\frac{Z\,dZ}{2-F-Z^2}\right)\frac{dZ}{2-F-Z^2}. \quad (88)\end{aligned}$$

Expansions are needed in the first and last terms on the right-hand side of (88). The arc lengths evaluated for the matched solutions for the 45° and 22·2° semi-angle wedges were underestimates of $0{\cdot}26\,Vt$ and $0{\cdot}05\,Vt$, respectively. (The approximate method of § 3 gave underestimates of 2·2 and 0·7.) The matching procedure described above therefore gives a satisfactorily close approximation.

The author wishes to express his great appreciation for many useful discussions with Prof. M. J. Lighthill and Dr R. F. Chisnell. The author also wishes to thank Mrs R. Grant for preparing the manuscript. The work was carried out while the author held a Department of Scientific and Industrial Research maintenance grant.

## REFERENCES

Cumberbatch, E. 1958 Ph.D. Thesis, Manchester University.
Garabedian, P. R. 1953 *Commun. Pure Appl. Math.* **6**, 157.
Wagner H. 1932 *Z. angew. Math. Mech.* **12**, 193.